Cell PRESS
Neuron
Article

The Extracellular Matrix Molecule Hyaluronic Acid Regulates Hippocampal Synaptic Plasticity by Modulating Postsynaptic L-Type Ca^{2+} Channels

Gaga Kochlamazashvili,[1,2,8] Christian Henneberger,[3,8] Olena Bukalo,[1,8] Elena Dvoretskova,[2] Oleg Senkov,[4,5] Patricia M.-J. Lievens,[2] Ruth Westenbroek,[6] Andreas K. Engel,[4] William A. Catterall,[6] Dmitri A. Rusakov,[3,*] Melitta Schachner,[1,7] and Alexander Dityatev[1,2,*]

[1]Zentrum für Molekulare Neurobiologie Hamburg, University Medical Center Hamburg-Eppendorf, Martinistrasse 85, Hamburg 20251, Germany
[2]Department of Neuroscience and Brain Technologies, Italian Institute of Technology, Morego 30, 16163 Genova, Italy
[3]UCL Institute of Neurology, University College London, Queen Square, London WC1N 3BG, UK
[4]Department of Neurophysiology and Pathophysiology, University Medical Center Hamburg-Eppendorf, Martinistrasse 52, Hamburg 20246, Germany
[5]Department of Clinical Neurobiology, University of Heidelberg, Heidelberg 69120, Germany
[6]Department of Pharmacology, University of Washington, F427 HSB, Seattle, WA 98195, USA
[7]Keck Center for Collaborative Neuroscience and Department of Cell Biology and Neuroscience, Rutgers University, 604 Allison Road, Piscataway, NJ 08854, USA
[8]These authors contributed equally to this work
*Correspondence: d.rusakov@ion.ucl.ac.uk (D.A.R.), alexander.dityatev@iit.it (A.D.)
DOI 10.1016/j.neuron.2010.05.030

SUMMARY

Although the extracellular matrix plays an important role in regulating use-dependent synaptic plasticity, the underlying molecular mechanisms are poorly understood. Here we examined the synaptic function of hyaluronic acid (HA), a major component of the extracellular matrix. Enzymatic removal of HA with hyaluronidase reduced nifedipine-sensitive whole-cell Ca^{2+} currents, decreased Ca^{2+} transients mediated by L-type voltage-dependent Ca^{2+} channels (L-VDCCs) in postsynaptic dendritic shafts and spines, and abolished an L-VDCC-dependent component of long-term potentiation (LTP) at the CA3-CA1 synapses in the hippocampus. Adding exogenous HA, either by bath perfusion or via local delivery near recorded synapses, completely rescued this LTP component. In a heterologous expression system, exogenous HA rapidly increased currents mediated by $Ca_v1.2$, but not $Ca_v1.3$, subunit-containing L-VDCCs, whereas intrahippocampal injection of hyaluronidase impaired contextual fear conditioning. Our observations unveil a previously unrecognized mechanism by which the perisynaptic extracellular matrix influences use-dependent synaptic plasticity through regulation of dendritic Ca^{2+} channels.

INTRODUCTION

Distinct aggregates of extracellular matrix (ECM) molecules surround cell bodies and proximal dendrites of some central neurons, forming the perineuronal nets. These aggregates are heterogeneous in their structure and composition, incorporating molecules secreted from both neurons and astrocytes (Brückner et al., 2003; Matthews et al., 2002). The structure of the perineuronal nets relies on a ternary molecular complex consisting of hyaluronic acid (HA), chondroitin sulfate proteoglycans of the aggrecan family, and tenascin-R (Galtrey and Fawcett, 2007; Yamaguchi, 2000). HA is a large, negatively charged, non-branched polymer composed of repeated disaccharides of glucuronic acid and *N*-acetylglucosamine. Multiple chondroitin sulfate-containing molecules can bind to a single molecule of HA, and all members of the chondroitin sulfate proteoglycan family of aggrecans bind to tenascin-R.

The role of ECM components of the perineuronal nets in modulating signal transfer throughout neural networks is only beginning to emerge. First, enzymatic removal of chondroitin sulfates (1) reduced long-term potentiation (LTP) at excitatory synapses in the hippocampal area CA1 (Bukalo et al., 2001), (2) disassembled the perineuronal nets while promoting ocular dominance plasticity and functional recovery in the damaged central nervous system in adult animals (Bradbury et al., 2002; Pizzorusso et al., 2002), and (3) increased the excitability of basket cells (Dityatev et al., 2007). Second, mice deficient in chondroitin sulfate proteoglycans, brevican, or neurocan showed impairments in LTP (Brakebusch et al., 2002; Zhou et al., 2001). Third, deficiency in tenascin-R also results in impaired LTP while reducing perisomatic GABAergic inhibition in the CA1 region (Saghatelyan et al., 2001).

These observations have suggested that two of the three major components of the perineuronal nets are involved in regulating GABAergic synaptic activity and LTP of excitatory transmission. Very recently, the third ECM component, HA, has been shown to affect both the mobility of α-amino-3-hydroxyl-5-methyl-4-isoxazolepropionate (AMPA) glutamate receptors

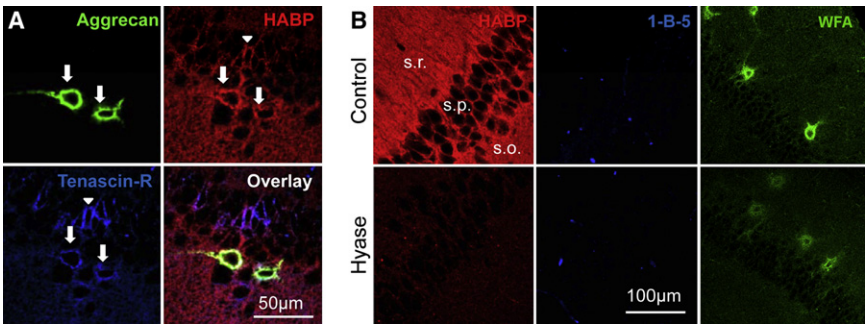

Figure 1. Expression of Hyaluronic Acid and Evidence for Its Removal by Hyaluronidase Treatment in the Hippocampal Slices

(A) Labeling of HA using biotinylated HABP shows the wide expression of HA in the hippocampus of the young adult mouse. HA is enriched in perineuronal nets around interneurons, which also contain aggrecan and tenascin-R (arrows) or tenascin-R only (arrowhead). "Overlay" panel shows colocalization of aggrecan, HA, and tenascin-R in white (all three molecules), yellow (aggrecan-HA), or purple (HA-tenascin-R).

(B) Treatment of slices with Hyase results in a loss of HABP signal and does not generate chondroitin sulfate stubs (1-B-5), which results from degradation of chondroitin sulfates. Labeling of perineuronal nets with WFA is partially preserved after Hyase treatment. The images shown in the top (control) and bottom (Hyase) panels were collected in different slices with the same acquisition parameters. The gain for acquisition of HABP signal is set higher in (B) than in (A) to increase sensitivity for detection of residual HA. s.r., s.p., and s.o. denote strata radiatum, strata pyramidale, and strata oriens, respectively. See also Figure S1.

and paired-pulse modulation in hippocampal cultures (Frischknecht et al., 2009). Here we find that in hippocampal slices from adult mice, HA not only modulates under certain conditions this form of short-term plasticity but also facilitates induction of LTP by increasing the activity of L-type voltage-dependent Ca^{2+} channels (L-VDCCs). Using a heterologous system, we identify the $Ca_V1.2$ subunit of L-VDCCs as a substrate for this potentiation by HA. Furthermore, removal of HA before fear conditioning impairs contextual fear memory, pointing to the functional importance of HA-rich ECM in the central nervous system.

RESULTS

Acute Removal of HA in Hippocampal Slices by Hyaluronidase

To investigate synaptic functions of HA, we used enzymatic pretreatment of acute hippocampal slices with hyaluronidase (Hyase). In untreated control slices, labeling with biotinylated HA binding protein (HABP) revealed a characteristic pattern of HA in the perineuronal nets containing aggrecan and/or tenascin-R (Figure 1A), consistent with previous observations (Brückner et al., 1993). In addition, widespread expression of HA was detected in the neuropil of strata radiatum and oriens (Figure 1; Figure 5). Treatment of slices with Hyase abolished the HABP signal both in the perineuronal nets and in the neuropil, thus confirming its specificity (Figure 1B; see Figure S5 available online). Expression of several major cytoskeletal, presynaptic, and postsynaptic proteins (actin α, tubulin III, subunits of L-VDCCs, glutamate, and $GABA_A$ receptors) remained unchanged after Hyase treatment (Figure S1). We also confirmed that this treatment did not remove chondroitin sulfates: immunostaining for the chondroitin sulfate stubs with the 1-B-5 antibody revealed no new stubs after Hyase treatment (Figure 1B). Labeling of the perineuronal nets with Wisteria floribunda agglutinin (WFA) was reduced after Hyase treatment (Figure 1B), presumably because some HA-associated components had become soluble after removal of HA. These results indicate that the enzyme can specifically and effectively cleave HA.

Hyaluronidase Treatment Impairs LTP but Has No Effect on Basal Synaptic Transmission or Paired-Pulse Facilitation

We next asked whether LTP induced by either weak or strong stimulation protocols, such as single or repetitive theta-burst stimulation (TBS) (Evers et al., 2002; Huber et al., 1995; Morgan and Teyler, 2001), would be influenced by HA. In Hyase-treated slices, single TBS induced LTP at a level indistinguishable from that in control conditions (Figures 2A and 2E). In contrast, the potentiation was reduced in Hyase-treated slices compared to control when the five TBS protocol was used (128.4% ± 2.7%, n = 11 and 148.8% ± 4.1%, n = 11, respectively; $p < 0.001$, unpaired t test; Figures 2B and 2E). Because Hyase did not reduce synaptic responses during TBS (Figure 2C), the effect is unlikely to involve reduction in postsynaptic excitation. Also, the observation that the single TBS LTP was intact after the Hyase treatment argued against the effects of Hyase on the NMDA receptor-dependent machinery of LTP induction. Furthermore, Hyase had no effect on the stimulus response curves (Figures S2A and S2B) or the paired-pulse facilitation in similar conditions (Figures S2C and S2D). A Hyase-dependent inhibition of paired-pulse depression reported earlier in cultures (Frischknecht et al., 2009) could be replicated in slices when the extracellular solution was modified to turn paired-pulse facilitation into depression (Figures S2E and S2F; Discussion).

Because the HA-containing perineuronal nets have previously been implicated in regulation of GABAergic activity (Dityatev et al., 2007; Saghatelyan et al., 2001), we tested whether such a mechanism could explain our observations. However, application of the $GABA_A$ receptor antagonist picrotoxin did not abrogate the difference in LTP between Hyase-treated and control slices (Figures 2D and 2E), thus effectively ruling out the involvement of GABAergic transmission in the effect of Hyase.

If the removal of HA by Hyase is responsible for the reduction of LTP, then reintroduction of HA in Hyase-treated slices should be able to restore LTP. We therefore washed out Hyase, incubated slices for 1 hr with HA, and induced LTP. This procedure effectively restored LTP (Figures 3A and 3D), indicating that the deficit in LTP after Hyase treatment is due to the absence of HA.

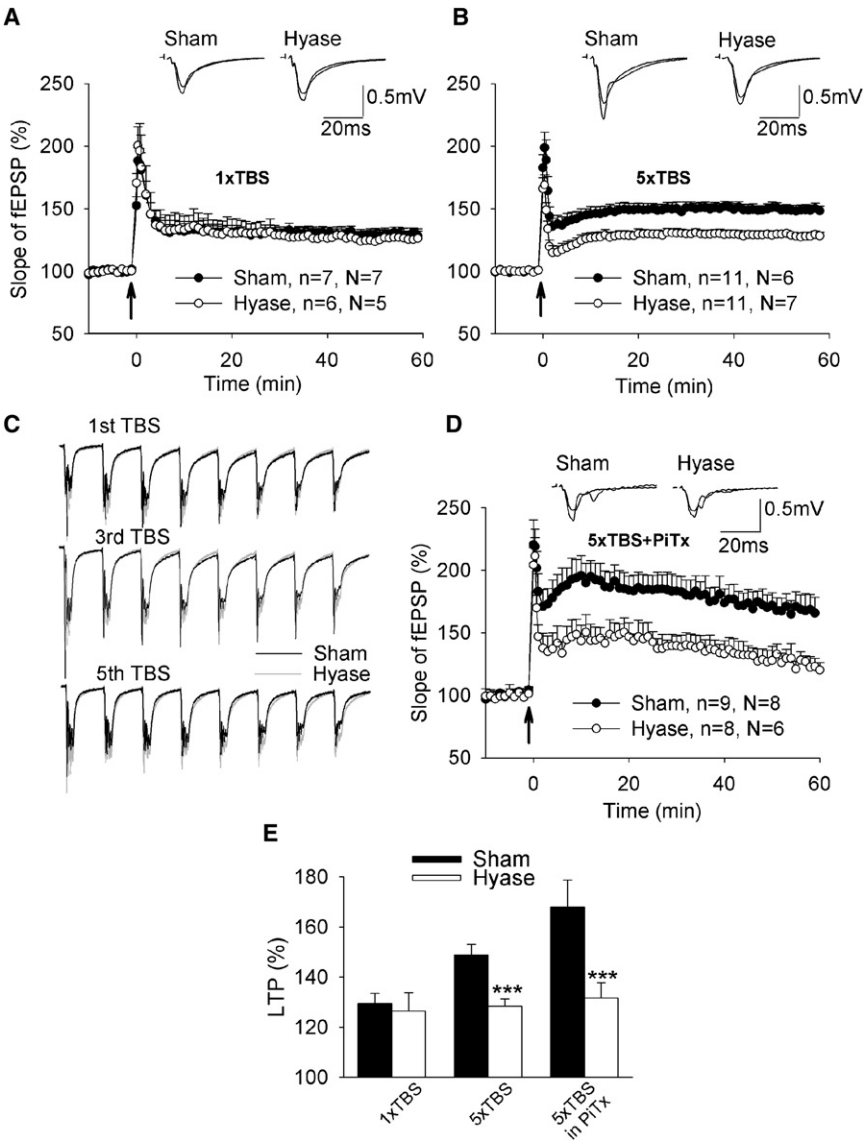

Figure 2. Hyaluronidase Treatment of Hippocampal Slices Reduces LTP, Depending on the Stimulation Protocol

(A) LTP induced by a single train of theta-burst stimulation (1×TBS) is normal after treatment with Hyase.

(B and D) LTP induced by five trains of theta-burst stimulation (5×TBS) is impaired after treatment with Hyase, irrespective of the absence (B) or presence (D) of 50 μM picrotoxin (PiTx). The mean slope of fEPSPs recorded 10 min before TBS was taken as 100%, and arrows indicate delivery of 1×TBS or 5×TBS, as indicated. Data represent means + standard error of the mean (SEM); n and N provide the numbers of tested slices and mice, respectively. Each trace is the average of 30 fEPSPs recorded 10 min before or 50–60 min after induction of LTP.

(C) Representative examples of responses elicited by the first, third, and fifth theta-burst stimulations in sham-treated (black) and Hyase-treated (gray) slices. The traces were normalized using the amplitude of fEPSP elicited by a single pulse.

(E) Means + SEM of LTP levels recorded 50–60 min after induction of LTP. ***$p < 0.001$, significant difference between control and Hyase-treated slices, unpaired t test. See also Figure S2.

Reduction in L-Type VDCC-Dependent Signaling Underlies Impairment of LTP in HA-Deficient Slices

Because the impairment of LTP in Hyase-treated slices occurs under the five, but not single, TBS protocol, mechanisms specifically recruited by the latter protocol could give rise to this impairment. It has been shown that L-VDCCs contribute to NMDA receptor-dependent LTP specifically during repetitive TBS (Evers et al., 2002; Huber et al., 1995; Morgan and Teyler, 2001; Raymond and Redman, 2002; Raymond and Redman, 2006). We therefore tested whether the involvement of L-VDCCs could explain the effect of Hyase on LTP induced by the five TBS protocol. Indeed, the levels of LTP seen in the presence of nifedipine, an antagonist of L-VDCCs, were indistinguishable between control and Hyase-treated slices (Figures 3B and 3D). These levels were also close to those observed in Hyase-treated slices without nifedipine (Figure 3D). Furthermore, potentiation of L-VDCCs with BAY K 8644 elevated LTP in Hyase-treated slices to the control level (Figures 3C and 3D). Hyase therefore had no effect on a nifedipine-insensitive component of NMDA receptor-dependent LTP while inhibiting a nifedipine-sensitive L-VDCC-mediated component. These observations suggest that other forms of LTP, which depend on L-VDCC, could be impaired by Hyase. Indeed, a well-documented L-VDCC-dependent form of LTP, which can be induced by spontaneous discharges of neurons in the presence of K^+ channel blocker tetraethylammonium (TEA) (Evers et al., 2002; Huber et al., 1995; Moosmang et al., 2005), was reduced in Hyase-treated slices (Figures S3A and S3B).

Because it has been suggested that in certain conditions L-VDCCs contribute to the expression, rather than induction, of LTP (Shinnick-Gallagher et al., 2003), we asked whether such a mechanism could be activated by our stimulation protocol. Application of nifedipine 10 min post induction had no effect on the level of LTP 40 min later, if compared to untreated controls (150.1% ± 3.1%, n = 6 and 148.8% ± 4.1%, n = 11, respectively; $p > 0.1$, unpaired t test; data not shown), thus confirming that in the present conditions L-VDCCs contribute mainly to the induction of LTP.

A previous study indicated that L-VDCCs could contribute to nuclear translocation of active extracellular signal-regulated kinases Erk1/2 and activation of the cyclic AMP response element-binding protein (CREB) after induction of LTP with

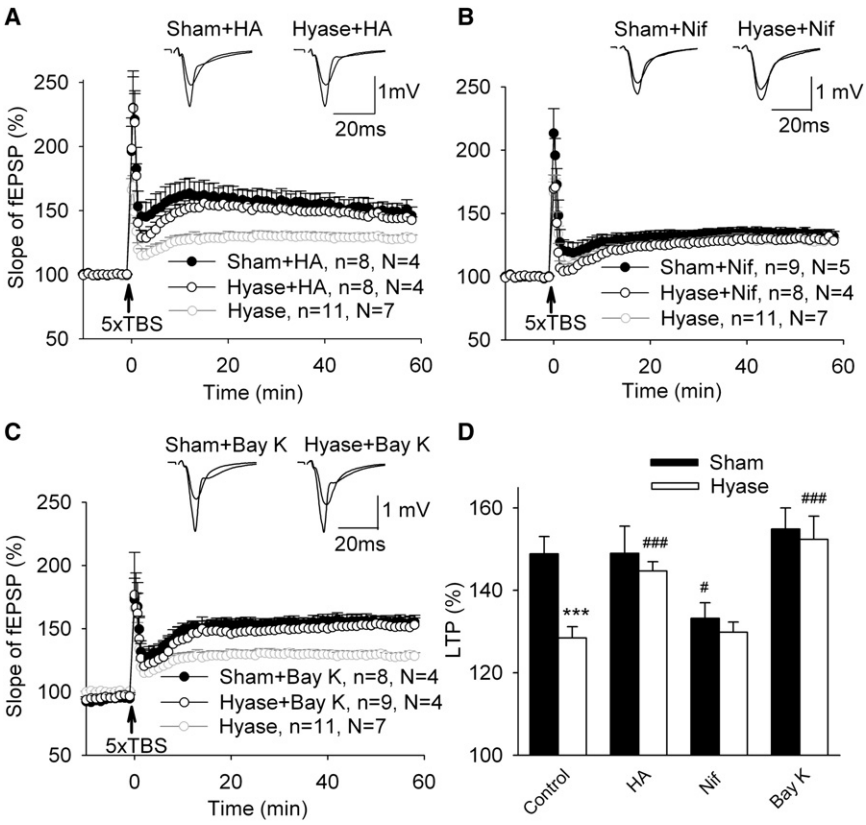

Figure 3. The Effect of Hyaluronidase on LTP Is Rescued by Hyaluronic Acid and Requires Activity of L-VDCCs

(A–C) The mean slope of fEPSPs recorded 10 min before 5×TBS was taken as 100%, and arrows indicate delivery of 5×TBS. Data represent means + SEM; n and N provide the numbers of tested slices and mice, respectively. Each trace is the average of 30 fEPSPs recorded 10 min before or 50–60 min after 5×TBS. To better illustrate effects of HA, nifedipine, and Bay K 8644, LTP recorded in Hyase-treated slices without these compounds is shown in gray.

(A) Restoration of impaired LTP in Hyase-treated slices by incubation with HA.

(B) LTP is reduced to the same levels in sham- and Hyase-treated slices in the presence of 10 μM nifedipine.

(C) LTP induced in Hyase-treated slices in the presence of 15 μM Bay K 8644 is restored to normal levels.

(D) Means + SEM of LTP levels recorded 50–60 min after 5×TBS. The bars show impaired LTP after Hyase and nifedipine treatments and restored LTP by HA or Bay K 8644 after Hyase treatment. ***$p < 0.001$, significant difference between control and Hyase-treated slices; $^{\#}p < 0.05$, significant effect of nifedipine on sham-treated slices; $^{\#\#\#}p < 0.001$, significant effects of HA and Bay K 8644 on Hyase-treated slices, unpaired t test. See also Figure S3.

TEA (Moosmang et al., 2005). Indeed, we found a significant upregulation of phosphorylated Erk1/2 and CREB in the CA1 stratum pyramidale in sham-treated, but not Hyase-treated, slices (Figures S3C–S3F). These data suggest that removal of HA impairs LTP-related signaling via Erk1/2 and CREB.

HA Potentiates L-VDCC Currents in a Heterologous Expression System

If Ca^{2+} currents through L-VDCCs are reduced by the removal of HA from the brain ECM, the addition of HA in a HA-free cell environment should enhance these currents. L-VDCCs in hippocampal neurons contain predominantly the pore-forming α_1 subunit $Ca_v1.2$. To directly demonstrate modulation of these channels by HA, we recorded currents mediated by $Ca_v1.2$ and auxiliary subunits β_1b and $\alpha_2\delta_1$ in transiently transfected Chinese hamster ovary (CHO) cells. A 4 min application of 100 μg/ml HA, but not vehicle alone, significantly potentiated L-VDCC currents within a wide range of holding voltages (Figures 4A–4F). The corresponding Boltzmann curves revealed that the maximal conductance, rather than voltage-dependent parameters, was affected by HA as compared to the vehicle (Figure 4E). In addition, application of 10 μg/ml HA potentiated L-VDCC to a lesser extent than did 100 μg/ml HA (Figure 4F), thus showing a concentration dependence of HA activity. There was no change in the inactivation of $Ca_v1.2$ channels after application of HA (Figure S4A).

Both α_1 and $\alpha_2\delta_1$, but not β_1, subunits of L-VDCC contain extracellular domains and thus might directly interact with HA. Interestingly, the α_2 subunit contains a von Willebrand A (VWA) domain (Davies et al., 2007). This domain is the most homologous to VWA domains found in inter-α-trypsin inhibitor heavy chains and collagens, which bind to HA (Bost et al., 1998; Specks et al., 1992). To evaluate whether the α_2 subunit of L-VDCC is responsible for modulation by HA, we compared modulation of L-VDCCs with and without $\alpha_2\delta_1$. The $\alpha_2\delta_1$-lacking channels were still potentiated by HA (Figure 4F), suggesting that HA modulation is mediated specifically by the α_1 subunit. To test whether HA also modulates currents mediated by $Ca_v1.3$, which is another α_1 subunit expressed in hippocampal neurons, we cotransfected CHO cells with $Ca_v1.3$ α_1, $\alpha_2\delta_1$, and β_1. The currents mediated by these channels were not affected by HA (Figure 4F; Figures S4B and S4C), thus indicating that HA specifically regulates $Ca_v1.2$-containing L-VDCCs.

HA in the CA1 Stratum Radiatum Contributes to LTP Induction

To verify that $Ca_v1.2$-containing L-VDCCs are expressed in the same subcellular compartments as HA, which is a precondition for their regulation by HA, a confocal microscopy analysis was performed. It revealed that HA was expressed in the vicinity of excitatory synapses in the stratum radiatum of the CA1 region (Figure 5A). Accumulations of HA were also associated with

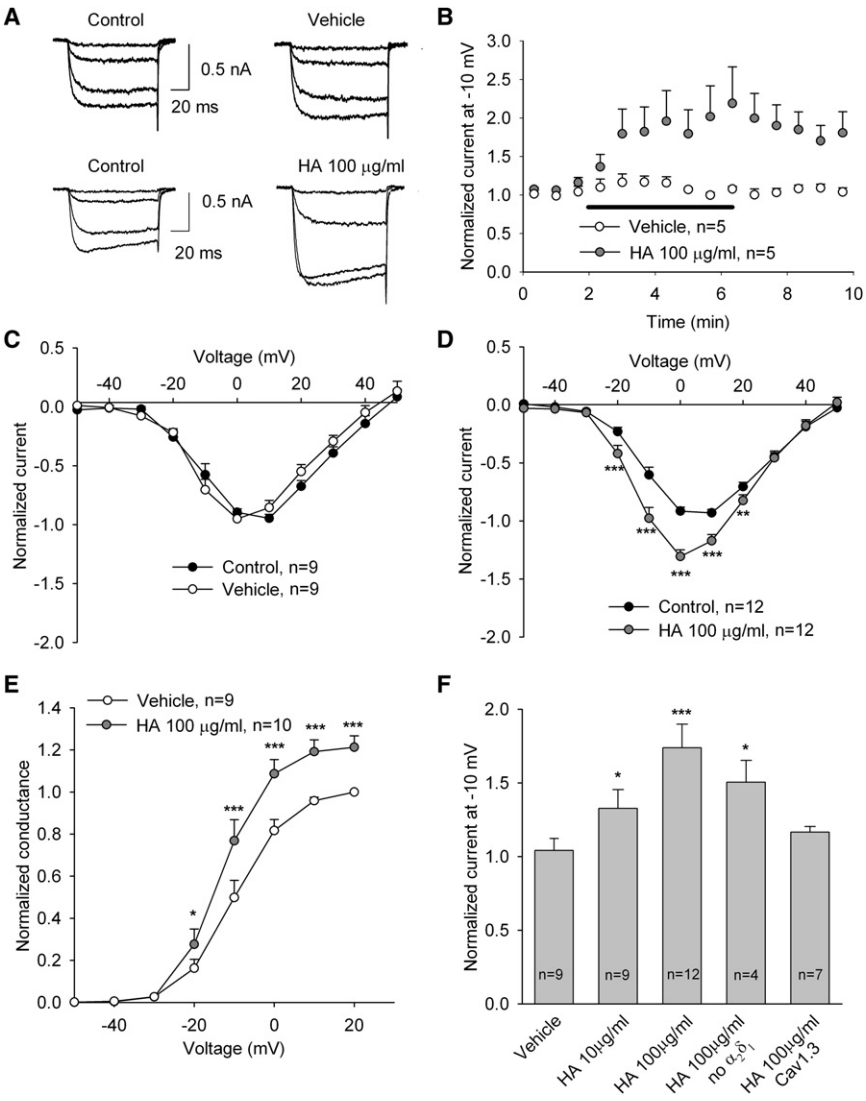

Figure 4. Potentiation of Cav1.2 L-VDCCs by HA in a Heterologous Expression System

(A) Representative recordings of currents in CHO cells transfected with $Ca_v1.2$ L-VDCCs 2 min after formation of whole-cell configuration (control) and 4 min after application of vehicle or 100 μg/ml HA. The currents shown were activated by voltage steps from −60 mV to −30, −20, −10, and 0 mV.

(B) The time course of changes in current activated at −10 mV. The mean amplitudes of currents recorded 80–100 ms after the beginning of voltage steps were measured and normalized using the baseline values.

(C and D) Mean current-voltage curves + SEMs. Individual current-voltage curves were first normalized to the respective maximal current amplitude in control conditions and then averaged.

(E) A difference between Boltzmann (mean + SEM) curves corresponding to currents recorded in the presence of 100 μg/ml HA or vehicle.

(F) A summary plot depicting the effects of 10 and 100 μg/ml HA on $Ca_v1.2$ channels with (bars 1–3) and without (bar 4) $\alpha_2\delta_1$ subunit, as well as on $Ca_v1.3$ channels (bar 5). Data represent mean + SEM of currents activated at −10 mV. *$p < 0.05$, **$p < 0.01$, ***$p < 0.001$, significant differences between control and HA-treated cells, paired t test (C and D) or significant differences between vehicle- and HA-treated cells, unpaired t test (E and F). See also Figure S4.

astroglial somata and processes (Figure 5B). Because optical resolution in these experiments ranged from ~0.3 μm (x-y plane) to ~0.8 μm (z axis), it was not possible to determine the precise subsynaptic location of HA. However, these data suggest that, on a submicron scale, the HA-based ECM tends to accumulate near astroglial and synaptic elements. Importantly, HA was expressed at the $Ca_v1.2$-immunopositive clusters on spines and dendrites in this region (Figure 5A; Figure S5; for comparison with previous immunostainings, see Hell et al., 1996), consistent with the hypothesis that HA may regulate the activity of L-VDCCs. At the same time, no apparent abnormality in the level of $Ca_v1.2$ expression (Figure S1) or the pattern of $Ca_v1.2$ immunoreactivity in the stratum radiatum (Figure S5B) was revealed after Hyase treatment.

Because both somatic and dendritic L-VDCCs have been reported to play a role in LTP (Lee et al., 2009; Raymond and Redman, 2006), we next asked whether modulation of dendritic L-VDCCs by perisynaptic HA is essential for LTP induced by the five TBS protocol. We found that local (visually controlled) injection of nifedipine near the dendritic recording site reduced LTP to the same level as bath application of the drug (Figures 6A, 6C, and 6E). Conversely, local injection of HA near the recording site in Hyase-treated slices (after washing out the enzyme) increased LTP to the level seen in control slices (Figures 6B, 6D, and 6E). These results associate HA modulation of dendritic L-VDCCs with the LTP component under study.

Hyaluronidase Reduces Ca^{2+} Influx through Postsynaptic L-VDCCs

To test more directly whether HA affects the functioning of neuronal L-VDCCs, we recorded Ca^{2+} currents in CA1 pyramidal neurons held in the whole-cell mode. These currents showed a much lower level of inhibition by nifedipine in Hyase-treated slices compared to control (inhibition by 5.7% ± 2.3%, n = 8, and by 18.7% ± 3.1%, n = 8, respectively; $p < 0.005$; Figure 7A), consistent with the suggestion that HA could affect LTP by regulating L-VDCCs (see above). At the same time, Hyase had no effect on the membrane potential, input resistance, rheobase, action potential generation (Table S1), or the spike adaptation pattern in CA1 pyramidal cells (Figures S6A–S6C), thus arguing against any effects on cell excitability.

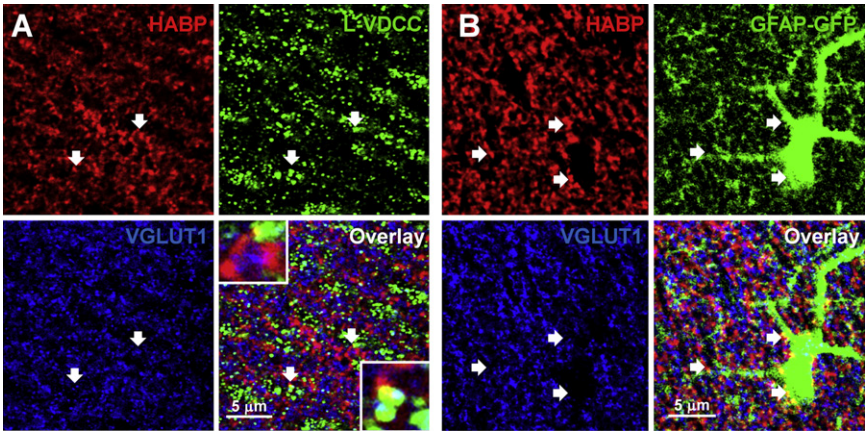

Figure 5. Hyaluronic Acid-Containing ECM Surrounds Excitatory Synapses, L-VDCC-Immunoreactive Dendrites, and Astrocytes in the Stratum Radiatum of CA1

(A) Labeling of HA using biotinylated HABP shows that HA appears as diffuse granular structures around L-VDCC-immunopositive clusters on dendrites (visible as dotted green stripes) or partially colocalizes with them. HA-containing structures surround the vast majority of VGLUT1-positive excitatory synapses. Two arrows point to clusters of L-VDCC immunoreactivity juxtaposed to VGLUT1-positive boutons and overlapping with HA-immunopositive areas, as shown with a higher magnification in insets.

(B) Association of HA-containing ECM with astrocytes (visualized by expression of GFP under the GFAP promoter). Arrows point to colocalization of HA-containing ECM and soma, proximal, and distal astrocytic processes. All images represent 0.8 μm thick optical sections. See also Figure S5.

To test whether the effects observed in whole-cell Ca^{2+} currents faithfully represent modulation of dendritic VDCCs, we filled CA1 pyramidal cells with the morphological tracer Alexa Fluor 594 and the Ca^{2+} indicator Fluo-4 (Figure 6F) and monitored Ca^{2+} transients evoked in dendritic spines and shafts by short trains of backpropagating action potentials, immediately before and 45 min after Hyase application (Figures 6F–6H; to achieve stability of Ca^{2+} recording over long time intervals during in situ drug application, these experiments had to be carried out in slices of 3- to 4-week-old rats). Again, to spatially restrict the action of Hyase, it was applied locally, near recorded dendritic spines through a patch pipette (Figure 6F). Alexa Fluor 594 was added to the pipette solution to monitor the diffusion profile of the ejected Hyase in the tissue, as described earlier (Rusakov et al., 2005). Application of Hyase reduced the postsynaptic Ca^{2+} responses by 33.4% ± 8.6% in dendritic spines ($n = 7$, $p < 0.001$) and by 42.7% ± 3.5% in dendritic shafts ($n = 8$, $p < 0.001$; the effect was indistinguishable between spines and shafts, $p > 0.3$; Figures 6G and 6H). Because a reduction in Ca^{2+} entry also results in altered conditions of postsynaptic Ca^{2+} buffering, diffusion, and removal, the effect of Hyase should thus lead to a changed spatiotemporal pattern of intracellular Ca^{2+} signaling. At the same time, Hyase had no effect on resting postsynaptic Ca^{2+} levels (Figures S6D–S6F; see Discussion for the relationship between these data and L-VDCC contribution to postsynaptic Ca^{2+} entry, reported earlier by Yasuda et al., 2003). Without Hyase application, Ca^{2+} signals integrated over the 600 ms interval remained unchanged for >45 min (sham condition, Figure 6G). If the effect of Hyase were mediated by L-VDCCs, it should be sensitive to blockade of L-VDCC activity. Indeed, preincubation of slices with nifedipine not only reduced the integrated spike-evoked Ca^{2+} entry but also occluded the inhibitory effect of Hyase treatment (Figure 6H). These results indicate that removal of HA reduces the activity of postsynaptic L-VDCCs in the CA1 region.

Hyaluronidase Reduces the Magnitude and Alters the Kinetics of Postsynaptic Ca^{2+} Influx Induced by TBS

To examine the effect of Hyase on postsynaptic L-VDCCs in conditions relevant to the induction of LTP, we recorded Ca^{2+} transients in dendritic spines of CA1 pyramidal cells (Figure 7B) in response to repetitive TBS of Schaffer collaterals (five theta trains 20 s apart, each consisting of eight high-frequency bursts, each including four stimuli at 100 Hz; Figure 7C). Again, the average Ca^{2+}-dependent signal evoked by a theta train was substantially reduced in Hyase-treated slices (Figure 7D). Furthermore, a multifactorial analysis of variance (three-way ANOVA) revealed that the removal of HA had changed the overall kinetics of postsynaptic Ca^{2+} entry in response to five theta trains (Figure 7E), which could be summarized as follows. In control conditions, the Ca^{2+} signal increment evoked by individual high-frequency bursts was decreasing both with the number of such bursts within trains ($p < 0.0001$) and with the number of theta trains ($p < 0.01$). Treatment with Hyase not only reduced Ca^{2+} signals throughout the stimuli ($p < 0.0001$) but also attenuated the use-dependent decrease of Ca^{2+} signals with the theta train numbers ($p < 0.01$ for interaction between theta train number and treatment; Figure 7E). The latter cannot be explained by indicator saturation, because the overall Ca^{2+} entry decreased by the treatment with Hyase. Our results therefore suggest that the presence of HA is important for setting both the magnitude (and therefore, spatiotemporal intracellular concentration landscape) and use-dependent adaptation of postsynaptic Ca^{2+} entry in response to multiple theta-burst stimuli.

Hyaluronidase Treatment Impairs Contextual Fear Conditioning

Previous studies reported the involvement of L-VDCCs in various aspects of fear conditioning (Bauer et al., 2002; Suzuki et al., 2004). To test whether removal of HA would affect contextual fear conditioning, we injected Hyase intrahippocampally 24 hr before carrying out a fear conditioning training (Figure 8A). Immunohistochemistry confirmed that this treatment effectively removed HA from the hippocampus for at least 24–72 hr (Figure S7). At the same time, the Hyase treatment affected neither the level of freezing before fear conditioning (Figure 8, B) nor the significant elevation of freezing between two unconditioned stimuli (Figure 8, S). The latter indicates that both vehicle- and

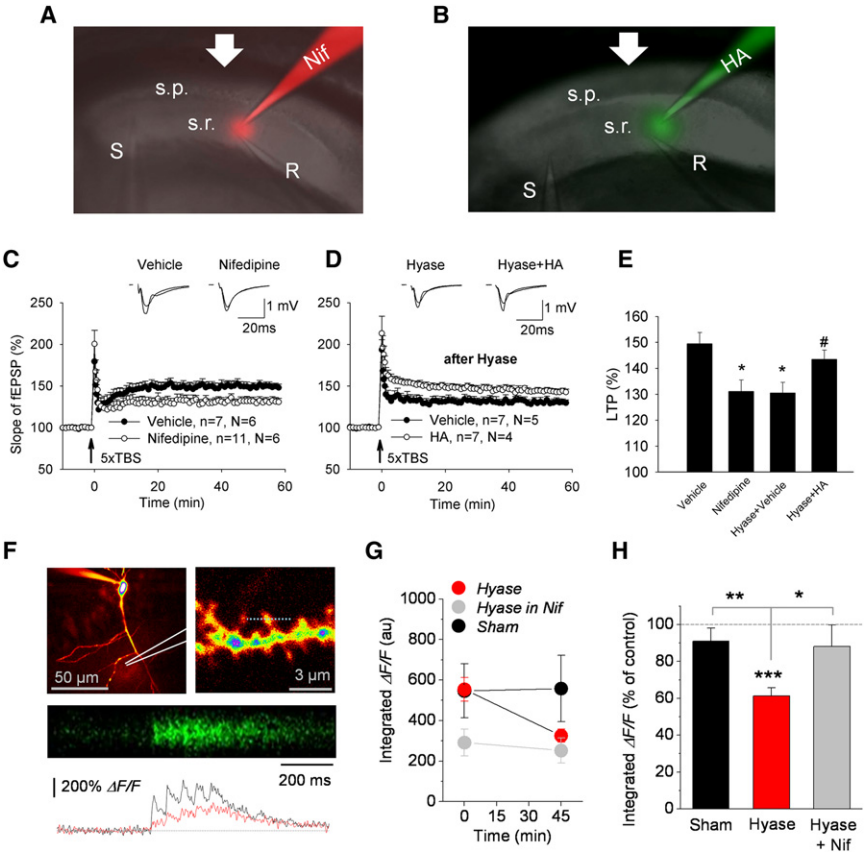

Figure 6. Dendritic Hyaluronic Acid Supports LTP and L-VDCC-Mediated Ca^{2+} Influx

(A and B) Location of stimulating (S) and recording (R) electrodes, injection pipettes with nifedipine (Nif) or HA, distribution of Alexa dye (coinjected with Nif in A), or fluorescein-conjugated HA (coinjected with unlabeled HA in B) in the stratum radiatum (s.r.). Note that there is no detectable dye in the stratum pyramidale (s.p.). Arrows indicate direction of perfusion with ACSF in the bath.

(C and D) The mean slope of fEPSPs recorded 10 min before 5×TBS was taken as 100%; arrows indicate delivery of 5×TBS. Data represent means + SEM; n and N provide the numbers of tested slices and mice, respectively. Each trace is the average of 30 fEPSPs recorded 10 min before or 50–60 min after 5×TBS.

(C) Impairment of LTP after injection of nifedipine.

(D) Restoration of impaired LTP in Hyase-treated slices by injection of HA. Note that a transient depression of fEPSPs (following theta-burst stimulation) was blocked after injection of HA, suggesting that an excess of HA might interfere with this short-term form of plasticity.

(E) Means + SEM of LTP levels recorded 50–60 min after 5×TBS. The bars show impaired LTP after nifedipine injection and restored LTP by HA injection after Hyase treatment. *$p < 0.05$, significant difference between vehicle and nifedipine or Hyase-treated slices; #$p < 0.05$, significant difference between vehicle and HA-injected Hyase-treated slices, unpaired t test.

(F) Top left: a characteristic recording configuration depicting a patch pipette (at the soma) and a pressure application pipette (dotted lines; the indicator ejection profile can be seen near the tip). Top right: a close-up on the dendritic fragment of interest. Middle: a characteristic line scan recording (line position above the dendritic fragment is shown at the top right) depicting the Ca^{2+} fluorescence response to five action potentials in control (average of five sweeps). Bottom: the global average line scan trace in control conditions (black) and 45 min after application of Hyase (red; n = 15 cells; experiments in slices from 3- to 4-week-old rats). See Figure S6G for other examples.

(G) The fluorescence signal $\Delta F/F$ integrated over the 1 s line scan interval (au, arbitrary units measured in raw traces) is stable in sham and nifedipine experiments but is reduced 45 min following Hyase application (means ± SEM before and after treatment are shown).

(H) Hyase treatment reduced Ca^{2+} responses in individual dendrites and spines (to 61.7% ± 4.4% of baseline, n = 15, ***$p < 0.0001$, one-population t test), whereas 10 µM nifedipine occluded this effect (88.0% ± 11.8% of baseline, n = 10, $p = 0.33$, difference with Hyase-only experiment at *$p < 0.05$, unpaired t test). The bars represent mean + SEM values. In control experiments, the fluorescence signal remains at 91.1% ± 6.9% of baseline over 45 min (sham control, n = 10, $p = 0.23$), which differs from the decreased signal following Hyase application (**$p < 0.01$). Note that the average relative change (normalized against the baseline, H) could differ slightly from the difference between absolute mean values measured in raw traces (G). See also Figure S6.

Hyase-injected groups equally perceived these stimuli. However, the freezing time in the conditioned context 24 hr after conditioning (Figure 8, d1) was smaller in the Hyase-injected group than in the group injected with the vehicle. This result suggests that the pretraining injection of Hyase impairs formation or retrieval of contextual fear memory.

DISCUSSION

The present study provides in vivo evidence for the functional importance of HA, a major component of the ECM in the central nervous system, for learning and/or memory and demonstrates that HA increases activity of L-VDCCs, thereby regulating LTP in hippocampal slices. We found that the removal of HA suppresses L-VDCC-mediated currents, reduces TBS-elicited Ca^{2+} transients in postsynaptic dendrites or spines, and abolishes an L-VDCC-dependent component of the TBS-induced LTP. The importance of HA for animal behavior is demonstrated by experiments in which pretraining injection of Hyase impaired fear conditioning.

Reintroduction of exogenous HA to Hyase-treated slices rescued LTP, thus suggesting a specific and reversible underlying mechanism. The specificity of the Hyase effects is also in accord with the unchanged expression of several key pre- and postsynaptic molecular players, as well as with the unaltered properties of basal synaptic transmission in Hyase-treated slices. The latter observations were, in general, consistent with the findings of a recent study in dissociated hippocampal cultures (Frischknecht et al., 2009). That study, however, also reported an increase in the paired-pulse ratio of excitatory postsynaptic currents paralleled by enhanced diffusion exchange between synaptic and extrasynaptic AMPA receptors following Hyase treatment. The apparent discrepancy could arise because, in acute slices, the synapses of interest normally

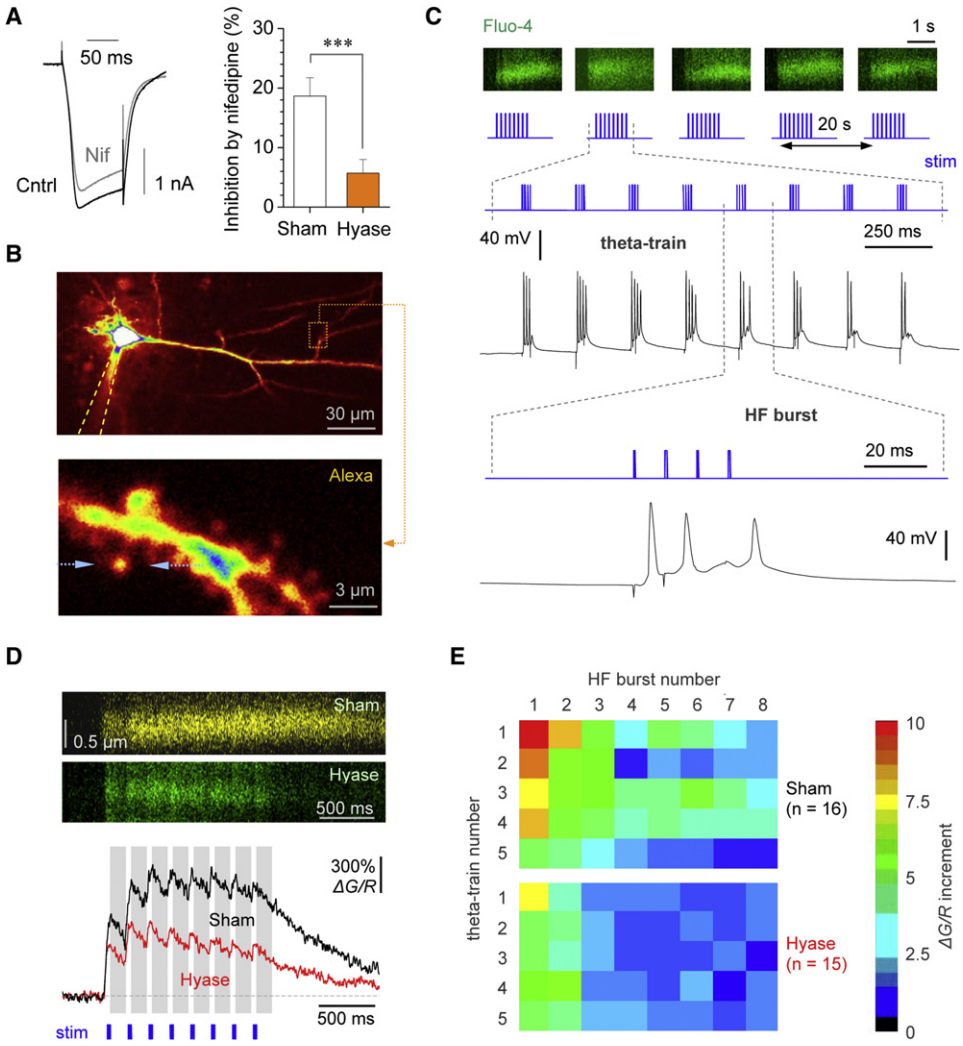

Figure 7. Enzymatic Cleavage of HA Reduces Nifedipine-Sensitive Currents, Decreases Overall Ca^{2+} Influx, and Alters Its Use-Dependent Kinetics during Theta-Burst Stimulation

(A) Left: a characteristic example of Ca^{2+} currents evoked by a voltage step from −80 to −20 mV before and after application of 10 µM nifedipine (Cntrl, black trace and Nif, gray trace, respectively) in a sham-treated slice. Right: a summary (mean + SEM) of Ca^{2+} current inhibition by nifedipine in sham- and Hyase-treated slices; ***$p < 0.005$ (unpaired t test, $n = 8$ in both groups).

(B) An example of a patched cell (top, a pipette indicated by dashed lines) with a selected dendritic fragment (dotted rectangle) zoomed in (bottom) as indicated (Alexa channel, dotted arrows, line scan position).

(C) Five TBS trains (rows 1 and 2) were delivered 20 s apart, each evoking a clear Ca^{2+} fluorescence transient (Fluo-4 channel) in the spine depicted in (B). Each TBS train (theta train) consisted of eight high-frequency bursts, each consisting of four stimuli at 100 Hz (row 3). Individual bursts evoked up to four action potentials in the postsynaptic cell (rows 4–6).

(D) Examples of the global average Ca^{2+} responses ($\Delta G/R$, corrected for focus drift in the "red" Alexa channel as described in the Experimental Procedures) in individual dendritic spines (top panels: average line scans at 500 Hz for single sample spines, Fluo-4 channel, false colors) in control conditions and following treatment with Hyase, as indicated. Grey columns in the traces depict the averaging time windows for the fluorescence signal measurements reflecting Ca^{2+} entry in response to individual high-frequency bursts. Stim denotes a depiction of the stimulation burst sequence.

(E) Color maps depicting the average incremental postsynaptic Ca^{2+}-dependent fluorescence signals (poststimulus increments representing $n = 945$ measurements in individual cells, as illustrated in D) in response to individual high-frequency bursts over five theta trains (each consisting of eight bursts), in control conditions and following Hyase treatment, as indicated. The three-way ANOVA was applied with respect to the factor levels corresponding to (1) the columns, (2) the rows, and (3) the two panels in each of $n = 31$ experiments. See Results, Experimental Procedures, and Supplemental Experimental Procedures for further details.

show paired-pulse facilitation, whereas in cultures they show paired-pulse depression, reflecting a substantially higher release probability compared to slices. This implies that in slices, the same synapse is unlikely to release glutamate twice in response to paired pulses, which in turn could mask use-dependent effects of receptor desensitization. Indeed, when we increased release probability in slices by elevating external Ca^{2+}, the ensuing paired-pulse depression was reduced by Hyase

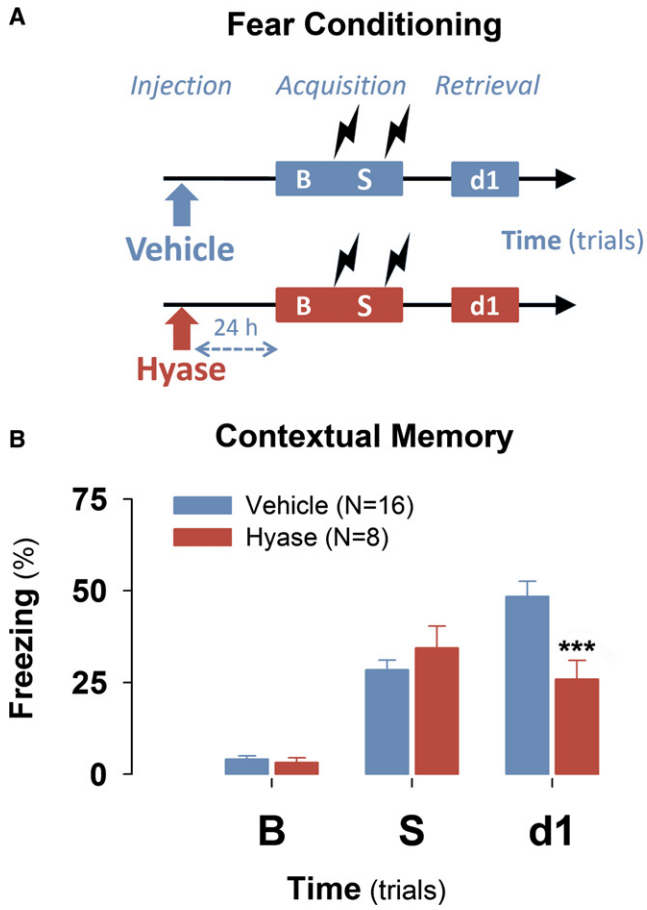

Figure 8. Intrahippocampal Injection of Hyaluronidase Impairs Contextual Fear Conditioning in Mice

(A) Scheme of experiments with intrahippocampal injections of Hyase or vehicle. B denotes baseline; S denotes time interval between unconditioned stimuli; d1 denotes memory retention test on posttraining day 1.

(B) Mean + SEM of freezing time before, during, and after fear conditioning for experimental groups shown in (A). ***$p < 0.001$, unpaired t test, significant differences in freezing between vehicle and Hyase-injected mice on posttraining day 1. Numbers of tested mice, N, are indicated in parentheses. See also Figure S7.

treatment (Figure S2E), consistent with the results reported in cultures (Frischknecht et al., 2009).

Because the deficit in LTP after removal of HA could not be rescued by blockade of GABAergic transmission, it is unlikely that any increases in the interneuron network activity are involved. This suggests that the mechanisms of plasticity impaired by Hyase are distinct from those affected by chondroitinase ABC or by the deficiency in tenascin-R (Bukalo et al., 2007; Dityatev et al., 2007; Saghatelyan et al., 2003). This is expected because an acute Hyase treatment does not lead to the full removal of chondroitin sulfates, as shown in the present study and earlier (Hedstrom et al., 2007). Furthermore, an acute chondroitinase ABC treatment does not fully remove HA in slices (unpublished data). Interestingly, HA removal produces the effects on CA1 LTP similar to those in the mice deficient in the ECM glycoprotein tenascin-C, which is expressed throughout the extrasynaptic space of the hippocampal neuropil, as seen by diffuse immunostaining. Here we report that HA, which is also expressed in the vicinity of synaptic structures, regulates postsynaptic Ca^{2+} signaling via L-VDCCs in the hippocampus. Because nifedipine had no effect on basal excitatory transmission or LTP expression, postsynaptic L-VDCCs are likely to contribute specifically to the induction of LTP in the CA1 region. Importantly, nifedipine reduced postsynaptic Ca^{2+} transients and its local application had a similar inhibitory effect on LTP, whereas local delivery of HA after Hyase treatment could restore LTP. These observations and the effect of Hyase on TBS-induced Ca^{2+} transients in spines and dendrites associate LTP induction in our study with predominantly dendritic HA and L-VDCCs. The latter is at variance with conclusions of an earlier study (Raymond and Redman, 2006) that implicated somatic rather than dendritic L-VDCCs in the late LTP. One possible reason for the apparent discord is that in the earlier study a high-affinity Ca^{2+} indicator was used for spine recordings, whereas a low-affinity one was used for somatic recordings; this might have led to dye saturation and therefore Ca^{2+} signal underestimation in spines (which we avoided by using Fluo-4 throughout).

In our experiments, the Hyase-sensitive, nifedipine-occluded component of dendritic Ca^{2+} signaling (30%–40%, Figures 6G and 6H) appears larger than the contribution of L-VDCCs to dendritic Ca^{2+} entry reported previously in baseline conditions (Yasuda et al., 2003). This might suggest that the effect of Hyase in our experiments involves Ca^{2+} signaling mechanisms that rely on L-VDCC activation rather than on Ca^{2+} influx through L-VDCCs, per se. Alternatively, this apparent discord might reflect the fact that both the L-VDCC-dependent Ca^{2+} entry and the efficiency of nifedipine are state and use dependent (Helton et al., 2005; Hoogland and Saggau, 2004) and therefore may vary substantially among experimental designs.

Hippocampal pyramidal neurons express predominantly the $Ca_v1.2$ subunit and relatively low levels of the $Ca_v1.3$ subunit. Accordingly, mice deficient in $Ca_v1.3$ channels show normal hippocampal LTP (Clark et al., 2003), whereas mice lacking the $Ca_v1.2$ channel exhibit impaired L-VDCC-dependent LTP (Moosmang et al., 2005). This is in agreement with expression of HA at $Ca_v1.2$-immunopositive clusters and with our experiments in the heterologous system, which demonstrated that HA modulates specifically $Ca_v1.2$ channels. The fact that the repetitive but not single TBS induces the L-VDCC-dependent form of LTP may reflect temporal summation of signaling events triggered by repeated stimuli and activity-dependent posttranslational modifications of L-VDCCs (one possible scenario is tyrosine phosphorylation and conversion of the long form of $Ca_v1.2$ subunit into the short form by proteolytic removal of the C terminus). Both of these modifications increase the activity of L-VDCCs (Calaghan et al., 2004; Gui et al., 2006; Hell et al., 1996; Le Blanc et al., 2004). Also, 12(*S*)-HPETE (12(*S*)-hydroperoxyeicosa-5*Z*,8*Z*,10*E*,14*Z*-tetraenoic acid), a downstream metabolite of the arachidonic acid-metabolizing enzyme 12-lipoxygenase, enhances postsynaptic somatodendritic Ca^{2+} influx through L-VDCCs during TBS (DeCostanzo et al., 2010).

As for the underlying molecular mechanism, our experiments with short-term application of HA to CHO cells suggest that

HA directly modulates the function of the $Ca_v1.2$ $\alpha1$ subunit of L-VDCCs (Figure 4B). This modulation cannot be mediated by the so-called link domain (Barta et al., 1993), which is similar to that of a C-type lectin (Kohda et al., 1996) and is present in most vertebral HA binding proteins but which is absent from all L-VDCC subunits. However, HA modulation of L-VDCCs may involve clusters of basic amino acids in the extracellular domain of the α_1 subunit, which appeared to mediate the potentiating effect on Ca^{2+} currents of another polyanionic glycosaminoglycan, heparin (Knaus et al., 1990). Further mutagenesis experiments are required to identify the precise HA interaction site(s).

In an attempt to understand the role of HA in hippocampus-dependent behavioral mechanisms, we found that the removal of HA had worsened animal performance in the contextual fear-conditioning paradigm. This observation highlights the importance of the ECM in memory formation and/or maintenance, in agreement with recent studies showing that removal of chondroitin sulfates or deficiency in tenascin-R, both of which are known to improve regeneration (Bradbury et al., 2002; Apostolova et al., 2006), also promotes formation of erasure-prone fear memories (Gogolla et al., 2009) and reversal learning (Morellini et al., 2010). Because HA remained absent during acquisition, consolidation, and retrieval of the contextual fear memory in our experiments, any of these processes may depend on HA, although L-VDCCs have been reported to contribute mainly to consolidation and reconsolidation of fear memories (Bauer et al., 2002; Suzuki et al., 2004). The latter is in line with our data showing a failure in L-VDCC-dependent activation of Erk1/2 and CREB in Hyase-treated hippocampal slices and the previously demonstrated role of Erk1/2 and CREB signaling in consolidation of contextual fear memories (Peters et al., 2009; Trifilieff et al., 2006). Interestingly, the acute removal of HA by Hyase resulted in a stronger impairment in fear conditioning as compared to tenascin-C- and $Ca_v1.2$-deficient mice (Moosmang et al., 2005; Morellini and Schachner, 2006), in which the deficits in signaling via L-VDCC could presumably be compensated during ontogenetic development and/or at the network level.

Our findings may shed light on the causal link between reported abnormalities in the HA expression and major neurological conditions. HA accumulates in demyelinated lesions in humans with multiple sclerosis and in mice with experimental autoimmune encephalomyelitis (Back et al., 2005 and references therein), in temporal cortex of patients with Alzheimer's disease (Jenkins and Bachelard, 1988), and in hippocampal tissue from patients with the temporal lobe epilepsy (Perosa et al., 2002). The potentiation of L-VDCCs by HA reported here is consistent with (1) the L-VDCC-dependent increase in intracellular Ca^{2+} concentration (Lopez et al., 2008) in the triple transgenic mouse model of Alzheimer's disease (Oddo et al., 2003) and (2) the anti-epileptic effects of L-VDCC blockers, including nifedipine, in clinical and experimental models of epilepsy (Otoom and Hasan, 2006; Triggle, 2006). Thus, our present findings suggest that inhibitors of hyaluronan synthases or other regulators of HA expression may affect epileptogenesis and cognitive functions in animal models of aging and Alzheimer's disease. In conclusion, our observations point to the mechanism by which HA may regulate synaptic functions in the normal central nervous system and, when abnormally accumulated, deregulate these essential functions and cause pathological changes characteristic for common neurological diseases.

EXPERIMENTAL PROCEDURES

Recordings of LTP and Immunohistochemistry

Two- to three-month-old C57BL/6J mice of both sexes were used for experiments. Preparation of hippocampal slices and extracellular recordings are described by Evers et al. (2002) and in the Supplemental Experimental Procedures.

To remove HA before recordings of LTP, slices were incubated for 2 hr at 35°C in 2 ml carbogen-infused ACSF supplemented with Hyase (from *Streptomyces hyalurolyticus*, Sigma H-1136; 70 U/ml), which cleaves β-GlcNAc-[1→4] glycosidic bonds yielding 4,5-unsaturated tetra- and hexasaccharides. Unlike other Hyases, this enzyme is specific for hyaluronic acid and does not cleave heparin, chondroitin, heparan, or chondroitin sulfates (Ohya and Kaneko, 1970). Slices incubated in 2 ml carbogen-infused ACSF without enzyme served as sham controls.

Local application of drugs to the stratum radiatum was performed using a glass pipette with a diameter of 4–5 μm that was attached to a 10 μl Hamilton syringe mounted on the UMP3 microsyringe injector and controlled by the UMC4 microprocessor controller (WPI). The distance between recording and injection pipette was approximately 50 μm. Injection started 20 min before induction of LTP and continued throughout the recording period. The rate of injection was 50 nl/min. The efficacy of drug delivery was established by injection of 500 μM D-2-amino-5-phosphonopentanoic acid (AP5), which reduced LTP to 1.9% ± 0.6% (n = 6, data not shown). To visualize the area of drug delivery, injection solution was supplemented with fluorescent compounds with molecular weight matching that of drugs. Thus, 10 μM Alexa Fluor 568 (Invitrogen) was added to 100 μM nifedipine containing ACSF, whereas fluorescein-conjugated HA (2.5 mg/ml, Sigma) was mixed with unlabeled HA (used in all other experiments) at a 1:1 ratio.

Labeling of HA and immunostaining of other ECM molecules, L-VDCCs, and presynaptic terminals is described elsewhere (Dityatev et al., 2007) and in the Supplemental Experimental Procedures.

Two-Photon Excitation Fluorescence Imaging

To examine TBS-evoked postsynaptic Ca^{2+} entry, acute 250 μm hippocampal slices from 7- to 8-week-old mice were prepared as described above, transferred to a submersion-type recording chamber (Scientific Systems Design), and superfused with (in mM): 124 NaCl, 2.5 KCl, 2 $CaCl_2$, 1.3 $MgSO_4$, 26 $NaHCO_3$, and 10 glucose bubbled with 95% O_2/5% CO_2 at room temperature. Acute 350 μm hippocampal slices from 3- to 4-week old male Sprague-Dawley rats were used to monitor Ca^{2+} transients evoked by backpropagating action potentials or injection of Hyase (in the presence of 50 μM D-APV at 33°C–35°C). The internal solution contained (in mM): 135 K methanesulfonate, 2 $MgCl_2$, 10 HEPES, 10 Na-phosphocreatine, 4 NaATP, 0.4 NaGTP, 0.03 Alexa Fluor 594 hydrazide sodium salt (Invitrogen), and 0.2 Fluo-4 pentapotassium salt (Invitrogen).

Imaging experiments were carried out using a Radiance 2100 imaging system (Zeiss-Biorad) linked to a femtosecond pulse laser MaiTai (Spectra-Physics-Newport) and were integrated with patch-clamp electrophysiology (Rusakov and Fine, 2003). Recording protocols and details of fluorescence data analyses are outlined in the Supplemental Experimental Procedures.

To evaluate Ca^{2+}-dependent responses to individual high-frequency bursts during a theta train, the incremental fluorescence signal amplitude was calculated by subtracting the decaying Ca^{2+} fluorescence arising from previous bursts (denoted "$\Delta G/R$ increment" in Figure 7E). Five theta trains 20 s apart, each containing eight high-frequency bursts (four stimuli at 100 Hz each) were applied to Schaffer collaterals, and the postsynaptic Ca^{2+} response was analyzed using a multifactorial variance analysis (three-way ANOVA) with the following factors: (1) theta train number, (2) burst number within a train, and (3) treatment with Hyase, as outlined in the Results.

Patch-Clamp Recording of Ca^{2+} Currents in Neurons

Ca^{2+} currents were recorded from CA1 pyramidal cells in Hyase-treated and control slices in (in mM): 95 NaCl, 25 tetraethylammonium chloride (TEACl), 2.5 KCl, 1.3 $MgSO_4$, 2 $CaCl_2$, 1 NaH_2PO_4, 26 $NaHCO_3$ and 10 glucose at room temperature. The intracellular solution contained (in mM): 125 CsCl, 20 TEACl, 10 HEPES, 5 MgATP, 0.3 NaGTP, and 5 EGTA; it adjusted to pH 7.2 using CsOH. Sodium currents and synaptic transmission were blocked by adding 1 μM TTX, 10 μM NBQX, 100 μM APV, and 100 μM picrotoxin to the extracellular solution. Calcium currents were elicited by 100 ms voltage steps from −80 mV to −20 mV and leak subtracted using the P/4 protocol.

Analysis of L-VDCC-Mediated Currents in a Heterologous Expression System

Recordings were performed in CHO-K1 cells maintained on plastic coverslips in 35 × 10 mm dishes in Dulbecco's modified Eagle's medium supplemented with 100 U/ml penicillin, 100 μg/ml streptomycin, 0.3 mg/ml L-glutamine, and 10% fetal bovine serum. Twenty-four hours before recordings, cells were transfected using Lipofectamine 2000. Plasmids encoding green fluorescent protein (GFP)-tagged $Ca_v1.3$ (0.6 μg, a gift from Joerg Striessnig from the University of Innsbruck, described by Koschak et al., 2001) or GFP (0.6 μg pmaxGFP, Amaxa) plus rat $Ca_v1.2$ (Snutch et al., 1991; pcDNA3 expression vector), together with rat β_1b and $\alpha_2\delta_1$ (pMT2 expression vector, 0.3 μg for each plasmid) were mixed with 100 μl Opti-MEM and then with 10 μl Lipofectamine 2000 diluted in 100 μl Opti-MEM. In some experiments, $\alpha_2\delta_1$ was omitted, as indicated in the text. The DNA-Lipofectamine 2000 complexes were applied to 50% confluent cell cultures for 4 hr. The medium was then exchanged with culture medium supplemented with Hyase (30 U/2.5 ml per well). Before recordings, cells were washed twice in extracellular solution containing (in mM): 120 NaCl, 10 HEPES, 10.8 $BaCl_2$, 1 $MgCl_2$, 5.4 CsCl, and 10 glucose (pH 7.4, adjusted with NaOH; Handrock et al., 1999). Whole-cell recordings were performed 24 hr after transfection using patch-clamp pipettes filled with intracellular solution containing (in mM): 120 CsCl, 5 HEPES, 3 $MgCl_2$, 10 EGTA, and 5 Mg-ATP (pH 7.3, adjusted with CsOH; Handrock et al., 1999). Patch pipettes (3–4 MΩ) were pulled from borosilicate glass (Hilgenberg). Currents were recorded with an EPC 10 USB Patch Clamp Amplifier (HEKA Elektronik). Data acquisition and command potentials were controlled by PATCHMASTER software (HEKA Elektronik), and data were stored for off-line analysis. To activate currents, 100 ms voltage steps were delivered at 10 s intervals, and leak and capacitive transients were digitally subtracted (Delling et al., 2002). Experiments were performed without knowing the identity of the substance applied: HA (10 or 100 μg/ml; Knaus et al., 1990) or vehicle (H_20).

Fear Conditioning

Thirty C57BL/6J male mice (2 to 3 months old) from Charles River Laboratories (Kisslegg, Germany) were used for the in vivo studies. Twenty-four mice were used for the behavioral tests, and six mice were used for pilot experiments to verify the in vivo effectiveness of Hyase injection for the duration of the fear conditioning test. The detailed description of the treatments is provided in the Supplemental Experimental Procedures. Mice were bilaterally injected with 2 U Hyase in 0.5 μl of sterile 0.9% NaCl per hippocampus 24 hr before fear conditioning. Freezing, which served as a measure of fear-related memory, was quantified as described previously (Senkov et al., 2006).

SUPPLEMENTAL INFORMATION

Supplemental Information includes Supplemental Experimental Procedures, one table, and seven figures and can be found online at doi:10.1016/j.neuron.2010.05.030.

ACKNOWLEDGMENTS

We thank Fabio Morellini and Kristin Michael for helpful suggestions, Tommaso Fellin for FVB/N-Tg(GFAPGFP)14Mes/J mice, and Joerg Striessnig for the $Ca_v1.3$ expression vector. This work was supported by the Deutsche Forschungsgemeinschaft (DI 702/6-1 to A.D.), the Italian Institute of Technology (G.K., P.M.-J.L., and A.D.), the Wellcome Trust and Medical Research Council UK (D.A.R. and C.H.), and the New Jersey Commission for Spinal Cord Research (M.S). M.S. is a consultant at the Center for Neuroscience at Shantou University Medical College, China.

Accepted: May 24, 2010
Published: July 14, 2010

REFERENCES

Apostolova, I., Irintchev, A., and Schachner, M. (2006). Tenascin-R restricts posttraumatic remodeling of motoneuron innervation and functional recovery after spinal cord injury in adult mice. J. Neurosci. *26*, 7849–7859.

Back, S.A., Tuohy, T.M., Chen, H., Wallingford, N., Craig, A., Struve, J., Luo, N.L., Banine, F., Liu, Y., Chang, A., et al. (2005). Hyaluronan accumulates in demyelinated lesions and inhibits oligodendrocyte progenitor maturation. Nat. Med. *11*, 966–972.

Barta, E., Deák, F., and Kiss, I. (1993). Evolution of the hyaluronan-binding module of link protein. Biochem. J. *292*, 947–949.

Bauer, E.P., Schafe, G.E., and LeDoux, J.E. (2002). NMDA receptors and L-type voltage-gated calcium channels contribute to long-term potentiation and different components of fear memory formation in the lateral amygdala. J. Neurosci. *22*, 5239–5249.

Bost, F., Diarra-Mehrpour, M., and Martin, J.P. (1998). Inter-alpha-trypsin inhibitor proteoglycan family—a group of proteins binding and stabilizing the extracellular matrix. Eur. J. Biochem. *252*, 339–346.

Bradbury, E.J., Moon, L.D., Popat, R.J., King, V.R., Bennett, G.S., Patel, P.N., Fawcett, J.W., and McMahon, S.B. (2002). Chondroitinase ABC promotes functional recovery after spinal cord injury. Nature *416*, 636–640.

Brakebusch, C., Seidenbecher, C.I., Asztely, F., Rauch, U., Matthies, H., Meyer, H., Krug, M., Böckers, T.M., Zhou, X., Kreutz, M.R., et al. (2002). Brevican-deficient mice display impaired hippocampal CA1 long-term potentiation but show no obvious deficits in learning and memory. Mol. Cell. Biol. *22*, 7417–7427.

Brückner, G., Brauer, K., Härtig, W., Wolff, J.R., Rickmann, M.J., Derouiche, A., Delpech, B., Girard, N., Oertel, W.H., and Reichenbach, A. (1993). Perineuronal nets provide a polyanionic, glia-associated form of microenvironment around certain neurons in many parts of the rat brain. Glia *8*, 183–200.

Brückner, G., Grosche, J., Hartlage-Rübsamen, M., Schmidt, S., and Schachner, M. (2003). Region and lamina-specific distribution of extracellular matrix proteoglycans, hyaluronan and tenascin-R in the mouse hippocampal formation. J. Chem. Neuroanat. *26*, 37–50.

Bukalo, O., Schachner, M., and Dityatev, A. (2001). Modification of extracellular matrix by enzymatic removal of chondroitin sulfate and by lack of tenascin-R differentially affects several forms of synaptic plasticity in the hippocampus. Neuroscience *104*, 359–369.

Bukalo, O., Schachner, M., and Dityatev, A. (2007). Hippocampal metaplasticity induced by deficiency in the extracellular matrix glycoprotein tenascin-R. J. Neurosci. *27*, 6019–6028.

Calaghan, S.C., Le Guennec, J.Y., and White, E. (2004). Cytoskeletal modulation of electrical and mechanical activity in cardiac myocytes. Prog. Biophys. Mol. Biol. *84*, 29–59.

Clark, N.C., Nagano, N., Kuenzi, F.M., Jarolimek, W., Huber, I., Walter, D., Wietzorrek, G., Boyce, S., Kullmann, D.M., Striessnig, J., and Seabrook, G.R. (2003). Neurological phenotype and synaptic function in mice lacking the CaV1.3 alpha subunit of neuronal L-type voltage-dependent Ca^{2+} channels. Neuroscience *120*, 435–442.

Davies, A., Hendrich, J., Van Minh, A.T., Wratten, J., Douglas, L., and Dolphin, A.C. (2007). Functional biology of the alpha(2)delta subunits of voltage-gated calcium channels. Trends Pharmacol. Sci. *28*, 220–228.

DeCostanzo, A.J., Voloshyna, I., Rosen, Z.B., Feinmark, S.J., and Siegelbaum, S.A. (2010). 12-Lipoxygenase regulates hippocampal long-term potentiation by modulating L-type Ca^{2+} channels. J. Neurosci. *30*, 1822–1831.

Delling, M., Wischmeyer, E., Dityatev, A., Sytnyk, V., Veh, R.W., Karschin, A., and Schachner, M. (2002). The neural cell adhesion molecule regulates

cell-surface delivery of G-protein-activated inwardly rectifying potassium channels via lipid rafts. J. Neurosci. *22*, 7154–7164.

Dityatev, A., Brückner, G., Dityateva, G., Grosche, J., Kleene, R., and Schachner, M. (2007). Activity-dependent formation and functions of chondroitin sulfate-rich extracellular matrix of perineuronal nets. Dev. Neurobiol. *67*, 570–588.

Evers, M.R., Salmen, B., Bukalo, O., Rollenhagen, A., Bösl, M.R., Morellini, F., Bartsch, U., Dityatev, A., and Schachner, M. (2002). Impairment of L-type Ca^{2+} channel-dependent forms of hippocampal synaptic plasticity in mice deficient in the extracellular matrix glycoprotein tenascin-C. J. Neurosci. *22*, 7177–7194.

Frischknecht, R., Heine, M., Perrais, D., Seidenbecher, C.I., Choquet, D., and Gundelfinger, E.D. (2009). Brain extracellular matrix affects AMPA receptor lateral mobility and short-term synaptic plasticity. Nat. Neurosci. *12*, 897–904.

Galtrey, C.M., and Fawcett, J.W. (2007). The role of chondroitin sulfate proteoglycans in regeneration and plasticity in the central nervous system. Brain Res. Rev. *54*, 1–18.

Gogolla, N., Caroni, P., Lüthi, A., and Herry, C. (2009). Perineuronal nets protect fear memories from erasure. Science *325*, 1258–1261.

Gui, P., Wu, X., Ling, S., Stotz, S.C., Winkfein, R.J., Wilson, E., Davis, G.E., Braun, A.P., Zamponi, G.W., and Davis, M.J. (2006). Integrin receptor activation triggers converging regulation of Cav1.2 calcium channels by c-Src and protein kinase A pathways. J. Biol. Chem. *281*, 14015–14025.

Handrock, R., Rao-Schymanski, R., Klugbauer, N., Hofmann, F., and Herzig, S. (1999). Dihydropyridine enantiomers block recombinant L-type Ca^{2+} channels by two different mechanisms. J. Physiol. *521*, 31–42.

Hedstrom, K.L., Xu, X., Ogawa, Y., Frischknecht, R., Seidenbecher, C.I., Shrager, P., and Rasband, M.N. (2007). Neurofascin assembles a specialized extracellular matrix at the axon initial segment. J. Cell Biol. *178*, 875–886.

Hell, J.W., Westenbroek, R.E., Breeze, L.J., Wang, K.K., Chavkin, C., and Catterall, W.A. (1996). N-methyl-D-aspartate receptor-induced proteolytic conversion of postsynaptic class C L-type calcium channels in hippocampal neurons. Proc. Natl. Acad. Sci. USA *93*, 3362–3367.

Helton, T.D., Xu, W., and Lipscombe, D. (2005). Neuronal L-type calcium channels open quickly and are inhibited slowly. J. Neurosci. *25*, 10247–10251.

Hoogland, T.M., and Saggau, P. (2004). Facilitation of L-type Ca^{2+} channels in dendritic spines by activation of beta2 adrenergic receptors. J. Neurosci. *24*, 8416–8427.

Huber, K.M., Mauk, M.D., and Kelly, P.T. (1995). Distinct LTP induction mechanisms: Contribution of NMDA receptors and voltage-dependent calcium channels. J. Neurophysiol. *73*, 270–279.

Jenkins, H.G., and Bachelard, H.S. (1988). Glycosaminoglycans in cortical autopsy samples from Alzheimer brain. J. Neurochem. *51*, 1641–1645.

Knaus, H.G., Scheffauer, F., Romanin, C., Schindler, H.G., and Glossmann, H. (1990). Heparin binds with high affinity to voltage-dependent L-type Ca^{2+} channels. Evidence for an agonistic action. J. Biol. Chem. *265*, 11156–11166.

Kohda, D., Morton, C.J., Parkar, A.A., Hatanaka, H., Inagaki, F.M., Campbell, I.D., and Day, A.J. (1996). Solution structure of the link module: A hyaluronan-binding domain involved in extracellular matrix stability and cell migration. Cell *86*, 767–775.

Koschak, A., Reimer, D., Huber, I., Grabner, M., Glossmann, H., Engel, J., and Striessnig, J. (2001). alpha 1D (Cav1.3) subunits can form l-type Ca^{2+} channels activating at negative voltages. J. Biol. Chem. *276*, 22100–22106.

Le Blanc, C., Mironneau, C., Barbot, C., Henaff, M., Bondeva, T., Wetzker, R., and Macrez, N. (2004). Regulation of vascular L-type Ca^{2+} channels by phosphatidylinositol 3,4,5-trisphosphate. Circ. Res. *95*, 300–307.

Lee, S.J., Escobedo-Lozoya, Y., Szatmari, E.M., and Yasuda, R. (2009). Activation of CaMKII in single dendritic spines during long-term potentiation. Nature *458*, 299–304.

Lopez, J.R., Lyckman, A., Oddo, S., Laferla, F.M., Querfurth, H.W., and Shtifman, A. (2008). Increased intraneuronal resting [Ca^{2+}] in adult Alzheimer's disease mice. J. Neurochem. *105*, 262–271.

Matthews, R.T., Kelly, G.M., Zerillo, C.A., Gray, G., Tiemeyer, M., and Hockfield, S. (2002). Aggrecan glycoforms contribute to the molecular heterogeneity of perineuronal nets. J. Neurosci. *22*, 7536–7547.

Moosmang, S., Haider, N., Klugbauer, N., Adelsberger, H., Langwieser, N., Müller, J., Stiess, M., Marais, E., Schulla, V., Lacinova, L., et al. (2005). Role of hippocampal Cav1.2 Ca^{2+} channels in NMDA receptor-independent synaptic plasticity and spatial memory. J. Neurosci. *25*, 9883–9892.

Morellini, F., and Schachner, M. (2006). Enhanced novelty-induced activity, reduced anxiety, delayed resynchronization to daylight reversal and weaker muscle strength in tenascin-C-deficient mice. Eur. J. Neurosci. *23*, 1255–1268.

Morellini, F., Sivukhina, E., Stoenica, L., Oulianova, E., Bukalo, O., Jakovcevski, I., Dityatev, A., Irintchev, A., and Schachner, M. (2010). Improved reversal learning and working memory and enhanced reactivity to novelty in mice with enhanced GABAergic innervation in the dentate gyrus. Cereb. Cortex. in press.

Morgan, S.L., and Teyler, T.J. (2001). Electrical stimuli patterned after the theta-rhythm induce multiple forms of LTP. J. Neurophysiol. *86*, 1289–1296.

Oddo, S., Caccamo, A., Shepherd, J.D., Murphy, M.P., Golde, T.E., Kayed, R., Metherate, R., Mattson, M.P., Akbari, Y., and LaFerla, F.M. (2003). Triple-transgenic model of Alzheimer's disease with plaques and tangles: Intracellular Abeta and synaptic dysfunction. Neuron *39*, 409–421.

Ohya, T., and Kaneko, Y. (1970). Novel hyaluronidase from streptomyces. Biochim. Biophys. Acta *198*, 607–609.

Otoom, S., and Hasan, Z. (2006). Nifedipine inhibits picrotoxin-induced seizure activity: Further evidence on the involvement of L-type calcium channel blockers in epilepsy. Fundam. Clin. Pharmacol. *20*, 115–119.

Perosa, S.R., Porcionatto, M.A., Cukiert, A., Martins, J.R., Amado, D., Nader, H.B., Cavalheiro, E.A., Leite, J.P., and Naffah-Mazzacoratti, M.G. (2002). Extracellular matrix components are altered in the hippocampus, cortex, and cerebrospinal fluid of patients with mesial temporal lobe epilepsy. Epilepsia *43* (*Suppl 5*), 159–161.

Peters, M., Bletsch, M., Catapano, R., Zhang, X., Tully, T., and Bourtchouladze, R. (2009). RNA interference in hippocampus demonstrates opposing roles for CREB and PP1alpha in contextual and temporal long-term memory. Genes Brain Behav. *8*, 320–329.

Pizzorusso, T., Medini, P., Berardi, N., Chierzi, S., Fawcett, J.W., and Maffei, L. (2002). Reactivation of ocular dominance plasticity in the adult visual cortex. Science *298*, 1248–1251.

Raymond, C.R., and Redman, S.J. (2002). Different calcium sources are narrowly tuned to the induction of different forms of LTP. J. Neurophysiol. *88*, 249–255.

Raymond, C.R., and Redman, S.J. (2006). Spatial segregation of neuronal calcium signals encodes different forms of LTP in rat hippocampus. J. Physiol. *570*, 97–111.

Rusakov, D.A., and Fine, A. (2003). Extracellular Ca^{2+} depletion contributes to fast activity-dependent modulation of synaptic transmission in the brain. Neuron *37*, 287–297.

Rusakov, D.A., Saitow, F., Lehre, K.P., and Konishi, S. (2005). Modulation of presynaptic Ca^{2+} entry by AMPA receptors at individual GABAergic synapses in the cerebellum. J. Neurosci. *25*, 4930–4940.

Saghatelyan, A.K., Dityatev, A., Schmidt, S., Schuster, T., Bartsch, U., and Schachner, M. (2001). Reduced perisomatic inhibition, increased excitatory transmission, and impaired long-term potentiation in mice deficient for the extracellular matrix glycoprotein tenascin-R. Mol. Cell. Neurosci. *17*, 226–240.

Saghatelyan, A.K., Snapyan, M., Gorissen, S., Meigel, I., Mosbacher, J., Kaupmann, K., Bettler, B., Kornilov, A.V., Nifantiev, N.E., Sakanyan, V., et al. (2003). Recognition molecule associated carbohydrate inhibits postsynaptic GABA(B) receptors: A mechanism for homeostatic regulation of GABA release in perisomatic synapses. Mol. Cell. Neurosci. *24*, 271–282.

Senkov, O., Sun, M., Weinhold, B., Gerardy-Schahn, R., Schachner, M., and Dityatev, A. (2006). Polysialylated neural cell adhesion molecule is involved in induction of long-term potentiation and memory acquisition and consolidation in a fear-conditioning paradigm. J. Neurosci. *26*, 10888–109898.

Shinnick-Gallagher, P., McKernan, M.G., Xie, J., and Zinebi, F. (2003). L-type voltage-gated calcium channels are involved in the in vivo and in vitro expression of fear conditioning. Ann. N Y Acad. Sci. *985*, 135–149.

Snutch, T.P., Tomlinson, W.J., Leonard, J.P., and Gilbert, M.M. (1991). Distinct calcium channels are generated by alternative splicing and are differentially expressed in the mammalian CNS. Neuron *7*, 45–57.

Specks, U., Mayer, U., Nischt, R., Spissinger, T., Mann, K., Timpl, R., Engel, J., and Chu, M.L. (1992). Structure of recombinant N-terminal globule of type VI collagen alpha 3 chain and its binding to heparin and hyaluronan. EMBO J. *11*, 4281–4290.

Suzuki, A., Josselyn, S.A., Frankland, P.W., Masushige, S., Silva, A.J., and Kida, S. (2004). Memory reconsolidation and extinction have distinct temporal and biochemical signatures. J. Neurosci. *24*, 4787–4795.

Trifilieff, P., Herry, C., Vanhoutte, P., Caboche, J., Desmedt, A., Riedel, G., Mons, N., and Micheau, J. (2006). Foreground contextual fear memory consolidation requires two independent phases of hippocampal ERK/CREB activation. Learn. Mem. *13*, 349–358.

Triggle, D.J. (2006). L-type calcium channels. Curr. Pharm. Des. *12*, 443–457.

Yamaguchi, Y. (2000). Lecticans: Organizers of the brain extracellular matrix. Cell. Mol. Life Sci. *57*, 276–289.

Yasuda, R., Sabatini, B.L., and Svoboda, K. (2003). Plasticity of calcium channels in dendritic spines. Nat. Neurosci. *6*, 948–955.

Zhou, X.H., Brakebusch, C., Matthies, H., Oohashi, T., Hirsch, E., Moser, M., Krug, M., Seidenbecher, C.I., Boeckers, T.M., Rauch, U., et al. (2001). Neurocan is dispensable for brain development. Mol. Cell. Biol. *21*, 5970–5978.